

## THERMAL EFFECTS IN ADIABATIC SHEAR BAND LOCALIZATION FAILURE

Piotr Perzyna (WARSAW)

The paper aims at the description of the influence of thermal effects on shear band localization failure. This kind of failure is generally attributed to a plastic instability generated by thermal softening during dynamic deformation. Basing on an analysis of the experimental results for dynamic loading the first stage of the dynamic flow process is treated as adiabatic. A thermo-elastic-plastic model of a material with internal micro-damage effects is used. Thermo-mechanical coupling is taken into consideration. A criterion for localization of the plastic deformation along shear band is investigated. Postcritical behaviour within shear bands is modelled by a thermo-elastic-viscoplastic response of a material with advanced microdamage process. Both models are developed within the framework of the rate type constitutive structure with internal state variables. The dynamic failure criterion within shear band is proposed. A simple micromechanical model of final failure with influence of thermal and anisotropic effects is presented.

### 1. Introduction

The main aim of the paper is to present a comprehensive description of the shear band localization failure within the thermodynamic framework of the rate type constitutive structure with internal state variables. Interpretation of the internal state variables introduced is given. To do this we based our consideration on discussion of recent experimental investigations concerning formation and developing of shear bands. This discussion is presented in chapter 2. Chapter 3 brings heuristic considerations concerning the dynamic process. A model of the description is proposed and the analysis of cooperative phenomena is presented.

In chapter 4 a thermo-elastic plastic model of damaged solids is developed. Rate type constitutive relation is formulated and the thermo-mechanical coupling effects are incorporated into the generalized heat conduction equation. Assuming adiabatic process and neglecting higher order terms the fundamental rate type equation is obtained. This result allows to use in the investigation of the criteria for localization along shear band the standard bifurcation method. Conditions for localization of plastic deformation give the critical hardening modulus rate and the orientation of the plane within which the shear band localization first takes place. Discussion of different effects on localization criteria is also given. Particular attention is focused on investigation of the influence of thermo-mechanical coupling effects as well as the micro-damage process.

Chapter 5 shows the constitutive modelling for the shear band region. Rate sensitivity, thermo-mechanical couplings, the strain induced anisotropy and the micro-damage mechanisms are taken into consideration.

Final failure along shear band region is discussed in chapter 6.

In chapter 7 the final comments and discussion of the theory developed are presented.

## 2. Discussion of experimental results

**2.1 Shear band formation and micro-damage process.** In dynamic loading processes failure may arise as a result of an adiabatic shear band localization generally attributed to a plastic instability generated by thermal softening during dynamic deformation.

Recent experimental observations (cf. GREBE, PAK and MEYERS [1985], HARTLEY, DUFFY and HAWLEY [1987], MARCHAND and DUFFY [1988], MARCHAND, CHO and DUFFY [1983] and CHO, CHI and DUFFY [1988]) have shown that the shear band procreates in a region of a body deformed where the resistance to plastic deformation is lower and the predisposition for band formation is higher.

GREBE, PAK and MEYERS 1985 were conducted ballistic impact experiments on 12.5 mm thick commercial purity titanium and T-6pct Al-4pct V alloy plates using

steel projectiles with 10.5 mm diameter. The impact velocities in their experiments varied between 578 m/s and 846 m/s. The microstructural damage mechanisms associated with shear band formation, shock wave propagation and dynamic fracture were investigated by optical and scanning and transmission electron microscopy. The shear bands were found along the two sides of the cross-section passing through the axis of the projectile. The measured shear band width in T6Al4V varied between 1 and 10  $\mu\text{m}$ . Observations of the onset of fracture along the shear band were also conducted. Spherical and ellipsoidal microcracks in T6Al4V were found along the bands. The mechanism of final failure in T6Al4V is a simple propagation of a macrocrack along the damaged material within the shear band region. In the explanation of the phenomenon of fracture along shear band very important role has the micro-damage process which consists of the nucleation, growth and coalescence of microvoids.

The investigations reported by GREBE, PAK and MEYERS 1985 indicated that in dynamic processes the shear band regions behave differently than adjacent zones. Within the shear band region the deformation process is characterized by very large strains (shear strains over 100%) and very high strain rates ( $10^3 - 10^5 \text{ s}^{-1}$ ). The strain rate sensitivity of a material becomes very important feature of the shear band region and the micro-damage process is intensified.

CHO, CHI and DUFFY 1988 performed microscopic observations of adiabatic shear bands in three different steels: an AISI cold rolled steel, HY-100 structural steel and AISI 4340 VAR steel subjected to two different heat treatments. Dynamic deformation in shear was imposed to produce shear bands in all the steels tested. It was found that whenever the shear band led to fracture of the specimen, the fracture occurred by a process of void nucleation, growth and coalescence. No cleavage was observed on any fracture surface, included the most brittle of the steel tested. The authors suggested that this is presumably due to softening of the shear band material that results from the local temperature rise occurring during dynamic deformation.

**2.2 Thermo-mechanical coupling effects.** HARTLEY, DUFFY and HAWLEY 1987, MARCHAND and DUFFY 1988 and MARCHAND, CHU and DUFFY 1988 presented the results of experiments in which the local strain and local temperature

$$L_{\nu}\tau \cong \dot{\tau}, L_{\nu}\mu \cong \dot{\mu}. \quad (4.28)$$

Let  $\mathbf{n}$  be the unit normal to the surface of a shear band across which certain components of the velocity gradient may admit jumps but remain uniform outside and inside the band. Let introduce rectangular Cartesian coordinate system  $\{x^i\}$  in such a way that  $\mathbf{n}$  is in the  $x_2$  - direction.

Superposition of the simplifications (i)-(iv) yields

$$\dot{\tau} = \mathbf{L}^{\#} \cdot \mathbf{d} \quad (4.29)$$

where

$$(\mathbf{L}^{\#})^{ijkl} = G(\delta^{ki}\delta^{lj}\delta^{kj}\delta^{il}) + (K - \frac{2}{3}G)\delta^{ij}\delta^{kl} \quad (4.30)$$

$$- \frac{G}{H + G + 9KA^2 - G\pi + 6GA\Xi} \left[ \frac{G}{\sqrt{J_2}} \tilde{\tau}'^{ij} + (3KA + 2G\Xi)\delta^{ij} \right] \left( \frac{G}{\sqrt{J_2}} \tilde{\tau}'^{kl} + 3KA\delta^{kl} \right),$$

with the denotations

$$\Pi = \frac{\chi(\sqrt{J_2} + AJ_1)\pi}{c_p G}, \Xi = \frac{3\theta K\chi(\sqrt{J_2} + J_1)}{2c_p G}. \quad (4.31)$$

The necessary condition for a localized shear band to be formed is

$$\det[\mathbf{L}^{\#2jk2}] = 0. \quad (4.32)$$

Substituting the matrix  $\mathbf{L}^{\#}$  into (4.32) we have

$$\frac{H_{cr}}{G} = -\frac{1+\nu}{2} \left( T + 2A + \frac{1-2\nu}{1+\nu} \Xi \right)^2 + \frac{(1-2\nu)^2}{1-\nu^2} \Xi^2 + \Pi,$$

$$\tan \delta = \left( \frac{S - T_{min}}{T_{max} - S} \right)^{\frac{1}{2}}, \quad (4.33)$$

where  $\delta$  denotes the angle between the vector  $\mathbf{n}$  and the  $\tilde{\tau}_{III}$  - direction, and the following denotations



were measured during the formation of an adiabatic shear band in an AISI 1018 cold rolled steel (CRS), and a low alloy structural steel (HY-100). In their experiments a torsional Kolsky bar was used to impose a rapid deformation rate in a short thin-walled tubular specimen. By testing a number of specimens they found that the plastic deformation process in the two steel tested can be divided into three separate stages. In the first stage, the shear strain is homogeneous both in the axial and in circumferential directions. This stage ends at a nominal strain of about 15% for CRS and 25% for HY-100 steel, which corresponds approximately to the maximum stress attained during the test for each kind of steel. With continued deformation, the strain distribution is no longer homogenous in the axial direction. During the second stage, which spans a range of nominal strains from 15% to 45% for CRS, and 25% to 50% for HY-100, there is a continuous increase in the magnitude of the localized strain in the axial direction. In this second stage the localized strain does not vary in the circumferential direction. As the nominal strain within this second stage increases, the localized strain increases to 150% for CRS, to 170% for HY-100 steel and the width of the band decreases from about 1100  $\mu\text{m}$  to 350  $\mu\text{m}$  for CRS, and 600  $\mu\text{m}$  to 150  $\mu\text{m}$  for HY-100 steel. In this stage of deformation, the flow stress level does not vary greatly. The third stage in the deformation process in each of two steel tested involves a sharp drop in stress, i.e. a loss in the load-carrying capacity of the material. Localized strains of up to 600% for CRS, and up to 1500% for HY-steel, and a corresponding of 100  $\mu\text{m}$  and of 20  $\mu\text{m}$  have been measured. The third stage continues until a crack appears within the shear band. This crack then propagates either part way or all the way around the specimen. It has been observed that, in the third stage, the deformation outside the band tends to a limit. The local temperature was determined by measuring the infrared radiation emanating from the specimen's surface, including the shear band area. It appears that the temperature rise occurs during the sharp decrease in the load-carrying capacity of the specimen for both of the two steels tested. In third stage the increase in local strain is associated with an increase of the local temperature from about 235°C to 575°C for CRS and about 460°C to 900°C for HY-100 steel.

**2.3 Strain rate sensitivity.** It is generally accepted that shear bands nucleate to the presence of a local inhomogeneity or defects, causing enhanced local deformation and heating. Once nonuniform flow procreates, the deformation becomes increasingly unstable as the dynamic process goes on if the heat that is produced during deformation is given insufficient time to be conducted away.

Experimental results have shown that localization occurs more readily in materials with a low strain hardening rate, a low strain rate sensitivity, a low thermal conductivity and a high thermal softening rate. Shear bands also form readily in high strength materials where the heat generated by plastic deformation is greater for a given plastic strain increment (cf. HARTLEY, DUFFY and HAWLEY 1987).

Along the shear band the deformation process is characterized by very intense strain and very large strain rates (cf. GREBE, PAK and MEYERS 1985 and HARTLEY, DUFFY and HAWLEY 1987). Strain rate sensitivity of a material becomes very important feature of the shear band region. It causes an increase in the flow stress with a corresponding decrease in ductility.

**2.4 Anisotropic effects.** Analysis of experimental results concerning investigations of adiabatic shear band localization failure under dynamic loading suggests that there are three main reason for anisotropic effects:

(i) The strain induced anisotropy is caused by the residual type stresses which result from the heterogeneous nature of the plastic deformation in polycrystalline materials (cf. IKEGAMI 1982 and PHILLIPS and LU 1984). Experimental evidence indicates that yield surfaces exhibit anisotropic hardening. Subsequent yield surfaces are both translated and deformed in stress space. In phenomenological description this kind of anisotropy is modelled by the shift of the yield surface in stress space. This shift of the yield surface might be described by the residual stress tensor  $\alpha$ .

(ii) The anisotropy caused by the formation of shear bands. This effect can be described by the determination of the direction of the shear band formed.

(iii) The anisotropy induced by the micro-damage process along the shear band region. Experimental observations (cf. YOKOBORI JR., YOKOBORI, SATO and SYOJI 1985, GREBE, PAK and MEYERS 1985 and HARTLEY, DUFFY and HAWLEY 1987) have shown that in the micro-damage process the generated anisotropy is

a consequence of rather random phenomena connected with some directional property of the formation of microcracks. This anisotropic effect is very much affected by the crystallographic structure of a material as well as by small fluctuations of main directions of the applied stress at particular point of a body during dynamic process.

To describe this kind of anisotropy one has to introduce an additional set of the internal state variables.

### 3. Heuristic consideration

**3.1 Analysis of cooperative phenomena.** An analysis of experimental results has clearly shown that the shear band localization failure in dynamic loading processes is affected by complex cooperative phenomena. From this analysis it is also evident that such cooperative phenomena as the thermo-mechanical flow process, the instability of the flow process along localized adiabatic shear bands, the micro-damage process which consists of the nucleation, growth and coalescence of microcracks and the final mechanism of failure are the most important for proper description of the fracture phenomenon under dynamic loading.

All these cooperative phenomena might be influenced by different additional effects such as the strain rate sensitivity, the induced anisotropy, the thermo-mechanical couplings and others.

It would be unrealistic to include in the description all effects observed experimentally. Constitutive modelling is understood as a reasonable choice of effects which are most important for explanation of the phenomenon described.

**3.2 Self-organization and physical interpretation of instability hierarchies.** We are interested in fracture phenomenon which is preceded by shear band localization. In this case the instability of the plastic flow process plays a fundamental role as a precursor of fracture .

Let consider a thermodynamic plastic flow process of a system (cf. Fig. 1). Synergetics suggests that a system is self-organized if it acquires a spatial, temporal or functional structure without specific interference from the outside. As a result of instability of plastic flow process we observe the macroscopic shear band pattern. A system has been self-organized in a new system - the shear band pattern system.

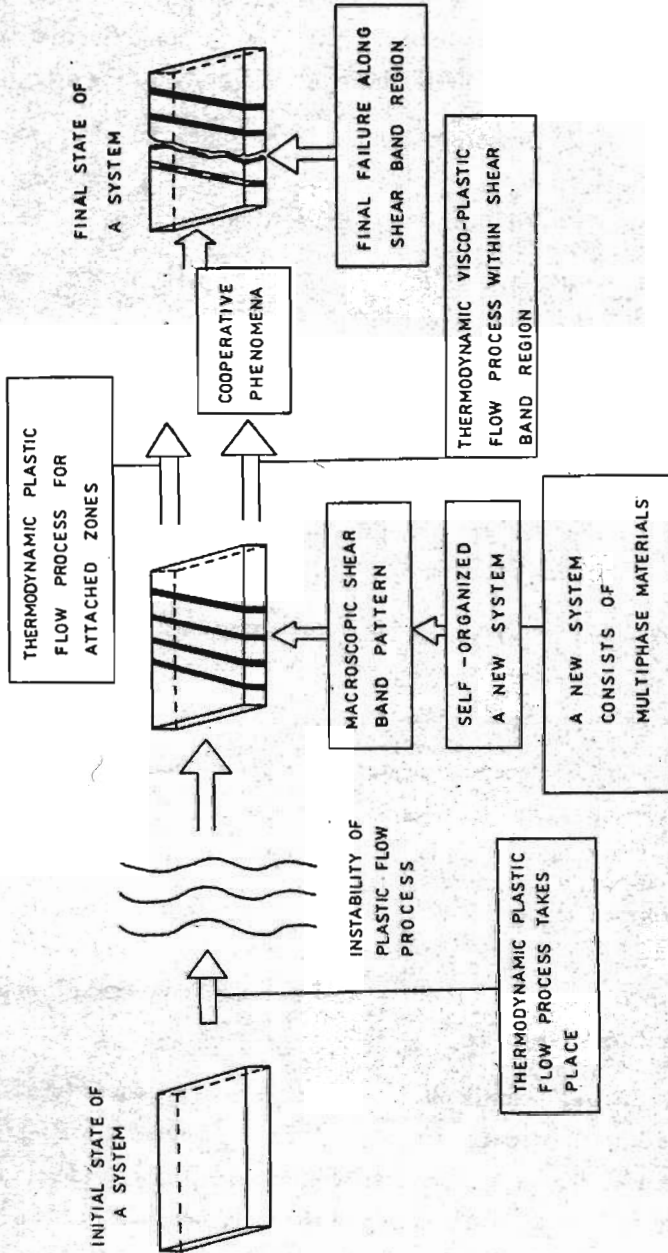


Fig.1



The instability phenomenon of plastic flow process can be considered at different levels. At the mesoscopic level we consider single crystals and their deformation. We describe the crystal lattice, consider movement of dislocations through the rows of barriers and take into account interactions of dislocations. At the macroscopic level by consideration of polycrystalline solids we are interested in description of the instability phenomenon of plastic flow processes. In particular we study the localization of plastic deformation along shear bands. So, we can expect the evolving macroscopic shear band pattern.

It seems that the study of instability hierarchies plays a very important role in the explanation of the interrelation between macroscopic deformation modes and dislocation structures evolved in single crystals (cf. NAKAYAMA and MORII [1987]).

**3.3 A model of the process.** It is postulated that during the first stage of the deformation process a thermo-elastic-plastic model of a material with internal micro-damage effects is utilized. The model accounts of thermo-mechanical couplings as well as of a combination of kinematic and isotropic hardening effects of a porous ductile, rate independent behaviour of a material.

At some instant of the process considered the adiabatic shear band localization may occur. So, a criterion for adiabatic shear band localization has to be investigated.

Along shear band region the localized plastic deformation process is very much influenced by strain rate sensitivity, the intrinsic macro-damage effects and thermo-mechanical couplings. The nucleation and growth mechanisms of microcracks become very important in this, stage of the dynamic deformation process. The micro-damage process is highly localized to the shear band region because the threshold stress for microcrack nucleation is much lower. This preferential nucleation is caused by higher temperature inside the shear band, with an attendant flow stress decrease. On the other hand the large plastic strain along the shear band region causes the intense growth of microcracks.

At some instant of the inelastic process the coalescence of microcracks begins. In this stage the fracture mechanism occurs. The coalescence of microcracks generates a macrocrack which propagates along the damaged shear band region and causes a final failure.

It is assumed that the response of a material along the shear band region is described by a thermo-elastic-viscoplastic model with very pronounced influence of the micro-damage process. The model takes account of thermo-mechanical couplings as well as of a combined kinematic and isotropic hardening of a porous ductile, rate sensitive plastic material.

The final failure of a body is described by a simple micromechanical model of the propagation of a macrocrack in damaged solid. The main idea of the model proposed is based on the experimental observations that the coalescence of microcracks can be treated as a nucleation and growth process on a smaller scale.

#### 4. Thermodynamic plastic flow process as a dynamical system

**4.1 General formulation.** We may treat our thermodynamic flow process as a dynamical system. Let  $\mathcal{A}(\mathbb{R}^+, \Psi)$  denote a set of the functions

$$\varphi = (\phi, \mathbf{v}, \vartheta, \boldsymbol{\mu}), \quad (4.1)$$

(where  $\phi$  is a motion,  $\mathbf{v}$  denotes the spatial velocity of the motion,  $\vartheta$  is temperature and  $\boldsymbol{\mu} \in V_n$  represents the internal state vector) defined on the set of non-negative real numbers  $\mathbb{R}^+$  with values in  $\Psi$ , i.e.

$$\varphi : \mathbb{R}^+ \rightarrow \Psi. \quad (4.2)$$

It will be convenient to introduce a nonlinear operator  $\mathbf{T}_{(\cdot)}$  such that

$$\varphi_\tau(t) = \varphi(\tau + t) = \mathbf{T}_{(\cdot)}\varphi(\tau), \tau \in \mathcal{T} \subset \mathbb{R}^+, t \in \mathbb{R}^+, \quad (4.3)$$

i.e.  $\varphi_\tau(t)$  is an element of  $\mathcal{A}(\mathbb{R}^+, \Psi)$  for any  $\varphi(\tau) \in \Psi_\tau$  and  $\mathbf{T}_{(\cdot)}$  is a mapping

$$\mathbf{T}_{(\cdot)} : \Psi \rightarrow \mathcal{A}(\mathbb{R}^+, \Psi). \quad (4.4)$$

For particular process the nonlinear operator  $\mathbf{T}_{(\cdot)}$  is defined by the initial - boundary value problem considered.

For a thermodynamic plastic flow process the mapping  $T_{(\cdot)}$  is defined by the initial - boundary - value problem as follows:

Find  $\phi, \mathbf{v}, \vartheta$  and  $\mu$  as function of  $x$  and  $t$  such that

(i) the field equations

$$\begin{aligned}
 \rho_{Ref} \dot{\mathbf{v}} &= \text{div} \boldsymbol{\tau}, \\
 L_{\mathbf{v}} \boldsymbol{\tau} &= \mathcal{L} \cdot \mathbf{d} - \mathcal{Z} \dot{\vartheta}, \\
 L_{\mathbf{v}} \boldsymbol{\mu} &= m(s) \left\langle \frac{1}{H} \{ \mathbf{P} : [\dot{\boldsymbol{\tau}} - (\mathbf{d} \cdot \boldsymbol{\alpha} + \boldsymbol{\alpha} \cdot \mathbf{d})] + \pi \dot{\vartheta} \} \right\rangle, \\
 \rho c_p \dot{\vartheta} &= \text{div}(k \text{grad} \vartheta) + \vartheta \frac{\rho}{\rho_{Ref}} \frac{\partial \boldsymbol{\tau}}{\partial \vartheta} : \mathbf{d} \\
 &\quad + \rho \chi \left\langle \frac{1}{H} \{ \mathbf{P} : [\dot{\boldsymbol{\tau}} - (\mathbf{d} \cdot \boldsymbol{\alpha} + \boldsymbol{\alpha} \cdot \mathbf{d})] + \pi \dot{\vartheta} \} \right\rangle;
 \end{aligned} \tag{4.5}$$

(ii) the boundary conditions

tractions  $(\boldsymbol{\tau} \cdot \mathbf{n})^a$  are prescribed on  $\partial B$ ,

temperature  $\vartheta$  is prescribed on  $\partial B$ ;

(iii) the initial conditions

$\phi, \mathbf{v}, \boldsymbol{\mu}$  and  $\vartheta$  are given at  $x \in B$  at  $t = 0$ ; are satisfied.

In the formulation of the initial-boundary-value problem the internal state vector  $\boldsymbol{\mu}$  is assumed as follows

$$\boldsymbol{\mu} = (\zeta, \boldsymbol{\alpha}, \xi), \tag{4.6}$$

where  $\zeta \in V_{n-7}$  the new internal state vector is introduced to describe the dissipation effects generated by plastic flow phenomena only,  $\boldsymbol{\alpha}$  is the residual stress (the back stress) and aims at the description of the kinematic hardening effects and  $\xi$  denotes the porosity or the volume fraction parameter brought in to take account of micro-damage effects.

The yield criterion has a particular form

$$f - \kappa = 0, \quad (4.7)$$

where

$$f = J_2 + [n_1(\vartheta) + n_2(\vartheta)\xi]J_1^2 \quad (4.8)$$

with

$$J_1 = \tilde{\tau}^{ab}g_{ab}, J_2 = \frac{1}{2}\tilde{\tau}'^{ab}\tilde{\tau}'^{cd}g_{ac}g_{bd}, \tilde{\tau} = \tau - \alpha, \quad (4.9)$$

$L_{\mathbf{v}}\tau$  denotes the Lie derivative of the Kirchhoff stress tensor  $\tau$ ,  $\mathbf{g}$  is the metric tensor in the current configuration,  $\kappa$  the isotropic hardening - softening parameter given by the material function

$$\begin{aligned} \kappa &= \hat{\kappa}(\epsilon^P, \vartheta, \xi) \\ &= [\kappa_1 + (\kappa_0 - \kappa_1)e^{-h(\vartheta)\epsilon^P}]^2 \left[1 - \frac{\xi}{\xi^F(\vartheta)}\right] (1 - b\bar{\vartheta}), \end{aligned} \quad (4.10)$$

$\kappa_0, \kappa_1$  and  $b$  are constants,

$$\bar{\vartheta} = \frac{\vartheta - \vartheta_0}{\vartheta_0}, \epsilon^P = \int_0^t \left(\frac{2}{3}\mathbf{d}^P : \mathbf{d}^P\right)^{\frac{1}{2}} dt, \quad (4.11)$$

$$\mathbf{d} = \mathbf{d}^e + \mathbf{d}^P, \quad (4.12)$$

$$H = H^* + H^{**}, \quad (4.13)$$

$$\begin{aligned} H^* &= -\frac{1}{2\sqrt{J_2}} \{n_1 J_1^2 + [\kappa_1 + (\kappa_0 - \kappa_1)e^{-h\epsilon^P}]^2 \frac{1 - b\bar{\vartheta}}{\xi^F} [k_1(\sqrt{J_2} + AJ_1) + 3Ak_2] \\ &\quad + \frac{h(\kappa_1 - \kappa_0)}{\sqrt{3J_2}} [\kappa_1 + (\kappa_0 - \kappa_1)e^{-h\epsilon^P}] \left[1 - \frac{\xi}{\xi^F}\right] (1 - b\bar{\vartheta})(1 + 6A^2)^{\frac{1}{2}} e^{-h\epsilon^P}, \end{aligned}$$

$$H^{**} = r\left(\frac{1}{2} + 3A^2\right), r = r_1 + r_2, \pi = \frac{1}{2\sqrt{J_2}} \frac{\partial \varphi}{\partial \vartheta},$$

$$\mathbf{P} = \frac{1}{2\sqrt{J_2}} \frac{\partial \varphi}{\partial \vartheta}, P_{ab} = \frac{1}{2\sqrt{J_2}} \tilde{\tau}'^{cd} g_{ca} g_{db} + A g_{ab},$$

$$A = \frac{1}{\sqrt{J_2}} (n_1 + n_2 \xi) J_1, k_1 = k_1(s), k_2 = k_2(s),$$

$$m(s) = \begin{cases} Z(s) \\ r_1 \mathbf{P} + r_2 \frac{\mathbf{P} : \mathbf{P}}{\tilde{\tau}' : \mathbf{P}} \tilde{\tau}, \\ k_1 \tilde{\tau} : \mathbf{P} + k_2 \mathbf{P} : \mathbf{g}, \end{cases}$$

and  $s$  denotes the intrinsic state which consists of a set of variables as follows

$$s = (\mathbf{e}, \mathbf{F}, \vartheta; \mu), \quad (4.14)$$

where  $\mathbf{e}$  denotes the Eulerian strain tensor and  $\mathbf{F}$  is the deformation gradient.

The conservation of mass gives

$$\rho_{Ref} = \rho_M^0(X)(1 - \xi_0) = \rho_M(1 - \xi)J(X, t) = \rho J(X, t), \quad (4.15)$$

where  $\rho_M$  is the mass density of the matrix material and  $J(X, t)$  denotes the Jacobian.

It is postulated that the free energy function exists and has the form

$$\psi = \hat{\psi}(s). \quad (4.16)$$

Finally the matrix  $\mathcal{L}$  and the tensor  $\mathcal{Z}$  have the form as follows

$$\begin{aligned} \mathcal{L} &= \left[ I - \frac{\frac{1}{H} \mathcal{L}^e \cdot \mathbf{P} \mathbf{P}}{1 + \frac{1}{H} (\mathcal{L}^e \cdot \mathbf{P}) : \mathbf{P}} \right] \cdot \left[ \mathcal{L}^e - \frac{1}{H} \mathcal{L}^e \cdot \mathbf{P} (\mathbf{P} \cdot \bar{\tau} + \bar{\tau} \cdot \mathbf{P}) \right], \\ \mathcal{Z} &= \left[ I - \frac{\frac{1}{H} \mathcal{L}^e \cdot \mathbf{P} \mathbf{P}}{1 + \frac{1}{H} (\mathcal{L}^e \cdot \mathbf{P}) : \mathbf{P}} \right] \cdot \left[ \mathcal{L}^{sh} - \frac{1}{H} \pi \mathcal{L}^e \cdot \mathbf{P} \right] \end{aligned} \quad (4.17)$$

where

$$\mathcal{L}^e = \rho_{Ref} \frac{\partial^2 \hat{\psi}}{\partial \mathbf{e}^2}, \quad \mathcal{L}^{sh} = -\rho_{Ref} \frac{\partial^2 \hat{\psi}}{\partial \mathbf{e} \partial \vartheta}. \quad (4.18)$$

the coefficient  $\chi$  and the specific heat  $c_p$  in the heat equation (4.5)<sub>4</sub> are determined by

$$\begin{aligned} \chi &= - \left[ \left( \frac{\partial \hat{\psi}}{\partial \xi} - \vartheta \frac{\partial^2 \hat{\psi}}{\partial \vartheta \partial \xi} \right) \cdot \mathcal{Z}(s) + \left( \frac{\partial \hat{\psi}}{\partial \alpha} - \vartheta \frac{\partial^2 \hat{\psi}}{\partial \vartheta \partial \alpha} \right) : \left( r_1 \mathbf{P} + r_2 \frac{\mathbf{P} : \mathbf{P}}{\bar{\tau} : \mathbf{P}} \bar{\tau} \right) \right. \\ &\quad \left. + \left( \frac{\partial \hat{\psi}}{\partial \xi} - \vartheta \frac{\partial^2 \hat{\psi}}{\partial \vartheta \partial \xi} \right) (k_1 \bar{\tau} : \mathbf{P} + k_2 \mathbf{P} : \mathbf{g}) \right], \quad c_p = -\vartheta \frac{\partial^2 \hat{\psi}}{\partial \vartheta^2}. \end{aligned} \quad (4.19)$$



We define the trajectory as the set of all pairs  $\{t, \varphi_\tau(t)\}$  for  $t \in \mathbb{R}^+$ , i.e. as a graph of the motion, cf. Fig. 2, and the orbit as the projection of the trajectory onto  $\Psi$ .

Let us consider the solution

$$\varphi_\tau(t) = \mathbf{T}_{(t)}\varphi(\tau) \in \mathcal{A}(\mathbb{R}^+, \Psi) \quad (4.20)$$

of the thermodynamic plastic flow process. For same  $\tau = \tau_c \in \mathcal{T}$  the solution  $\varphi$  can be not unique. Starting from the point  $\{\tau_c, \varphi_\tau(\tau_c)\}$  on the trajectory we can expect more than one solution (cf. Fig. 2).

So, we have at  $\{\tau_c, \varphi_\tau(\tau_c)\}$  branching of the solution. In other words the mapping  $\mathbf{T}_{(\cdot)}$  is a non-single-valued function (is a multi-function).

**4.2 Quasi-static and adiabatic approximation.** In many practical situations the thermodynamic plastic flow process can be treated as quasi-static and adiabatic.

Then the mapping  $\mathbf{T}_{(\cdot)}^*$  is defined by the following initial-boundary-value problem:

Find  $\varphi = (\phi, \mathbf{v}, \vartheta, \mu)$  as function of  $x$  and  $t$  such that

(i) the field equations

$$\begin{aligned} \operatorname{div} \tau &= 0, \\ L_v \tau &= \mathcal{L} \cdot \mathbf{d} - \mathcal{Z} \dot{\vartheta}, \\ L_r \mu &= m(s) \left\langle \frac{1}{H} \{ \mathbf{P} : [\dot{\tau} - (\mathbf{d} \cdot \boldsymbol{\alpha} + \boldsymbol{\alpha} \cdot \mathbf{d})] + \pi \dot{\vartheta} \} \right\rangle, \\ c_p \dot{\vartheta} &= \frac{\vartheta}{\rho_{Ref}} \frac{\partial \tau}{\partial \vartheta} : \mathbf{d} + \chi \left\langle \frac{1}{H} \{ \mathbf{P} : [\dot{\tau} - (\mathbf{d} \cdot \boldsymbol{\alpha} + \boldsymbol{\alpha} \cdot \mathbf{d})] + \pi \dot{\vartheta} \} \right\rangle, \end{aligned} \quad (4.21)$$

(ii) traction  $(\tau \cdot \mathbf{n})^a$  are prescribed on  $\partial B$ ,

temperature  $\vartheta$  is prescribed on  $\partial B$ ;

(iii)  $\phi, \mathbf{v}, \mu$  and  $\vartheta$  are given at  $X \in B$  at  $t = 0$ ;

are satisfied.

For adiabatic plastic flow process the evolution equation for temperature can be written in the form

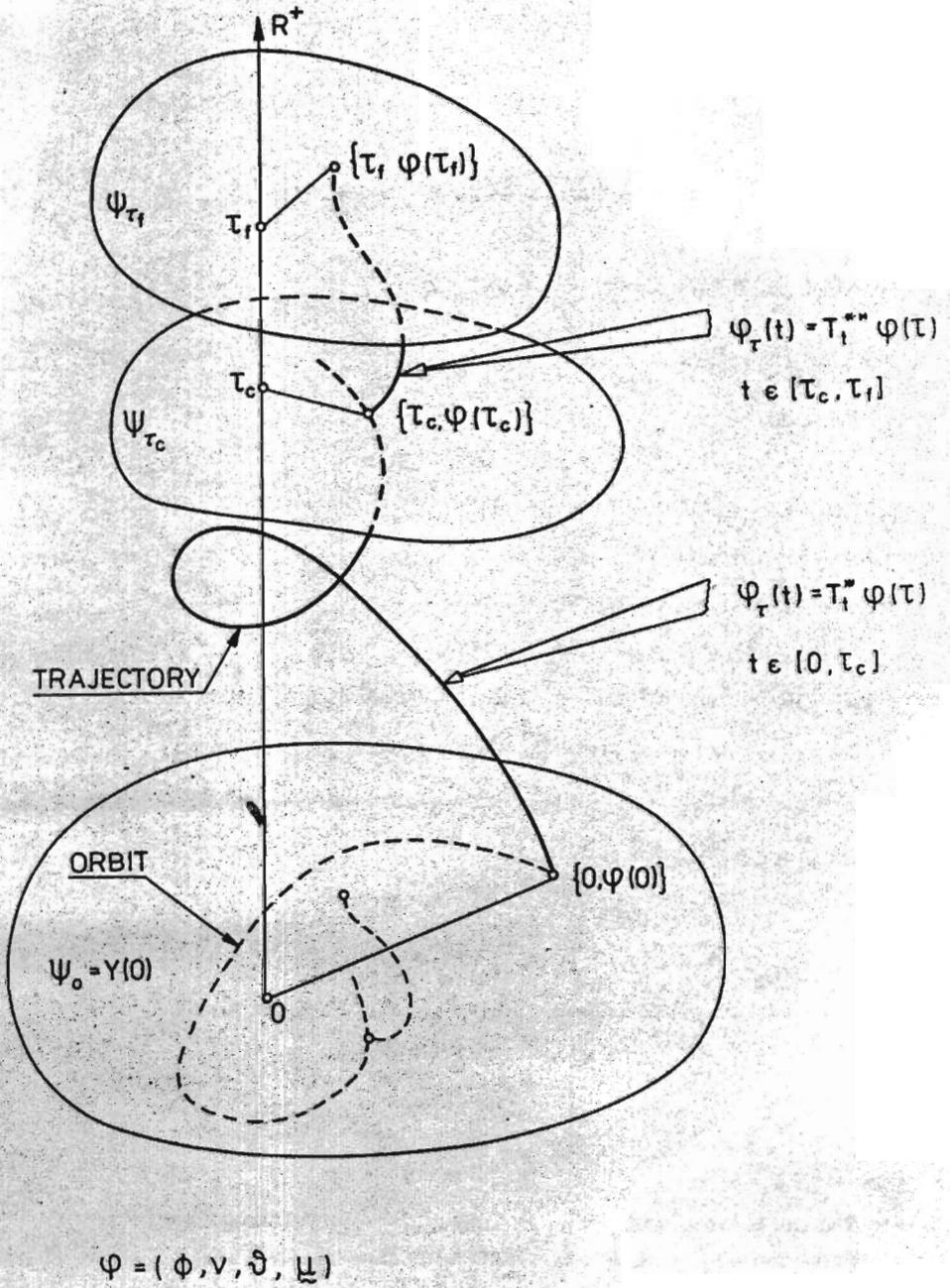


Fig. 2

$$\dot{\vartheta} = M : L_{\nu}\tau + N : d, \quad (4.22)$$

where

$$M = \frac{\chi P}{H c_p - \chi \pi}, N = \left[ \frac{\partial H}{\rho_{Ref}} \frac{\partial \tau}{\partial \vartheta} + \chi (P \cdot \tilde{\tau} + \tilde{\tau} \cdot P) \right] (H c_p - \chi \pi)^{-1}. \quad (4.23)$$

Substituting (4.22) into (4.21)<sub>2</sub> gives

$$L_{\nu}\tau = L \cdot d, \quad (4.24)$$

where

$$L = \left( I - \frac{\mathcal{Z}M}{1 + \mathcal{Z} : M} \right) \cdot (\mathcal{L} - \mathcal{Z}N). \quad (4.25)$$

The last results allows to use in the investigation of criteria for localization along shear band the standard bifurcation method.

**4.3 Criteria for shear band localization.** To make possible analytical investigation of criteria for localization we introduce some simplifications.

- (i) the second order terms in Eq.(4.22) are neglected. It means that only main contribution to thermo-mechanical couplings is taken into consideration.
- (ii) By analogy with the infinitesimal theory of elasticity we postulate

$$(\mathcal{L}^e)^{abcd} = G(g^{ca}g^{db} + g^{cb}g^{da}) + (K - \frac{2}{3}G)g^{ba}g^{cd}, \quad (4.26)$$

where  $G$  and  $K$  denote the shear and bulk modulus, respectively.

It is assumed that

$$\mathcal{L}^{e^{-1}} \cdot \mathcal{L}^{th} = \theta g, \quad (4.27)$$

where  $\theta$  is the thermal expansion coefficient.

- (iv) To concentrate discussion on the influence of thermo-mechanical coupling and the micro-damage effects on criteria for localization it will be convenient to neglect the spacial covariance terms by assuming

$$\begin{aligned}
 S &= -(1 - \nu)T + 2(1 + \nu)\Xi + (1 - 2\nu)\Xi, & (4.34) \\
 T_{max} &= \frac{\bar{\tau}_I'}{\sqrt{J_2}}, \quad T = \frac{\bar{\tau}_{II}'}{\sqrt{J_2}}, \quad T_{min} = \frac{\bar{\tau}_{III}'}{\sqrt{J_2}}, \\
 \nu &= \frac{3K - 2G}{2(3K + G)},
 \end{aligned}$$

are introduced.

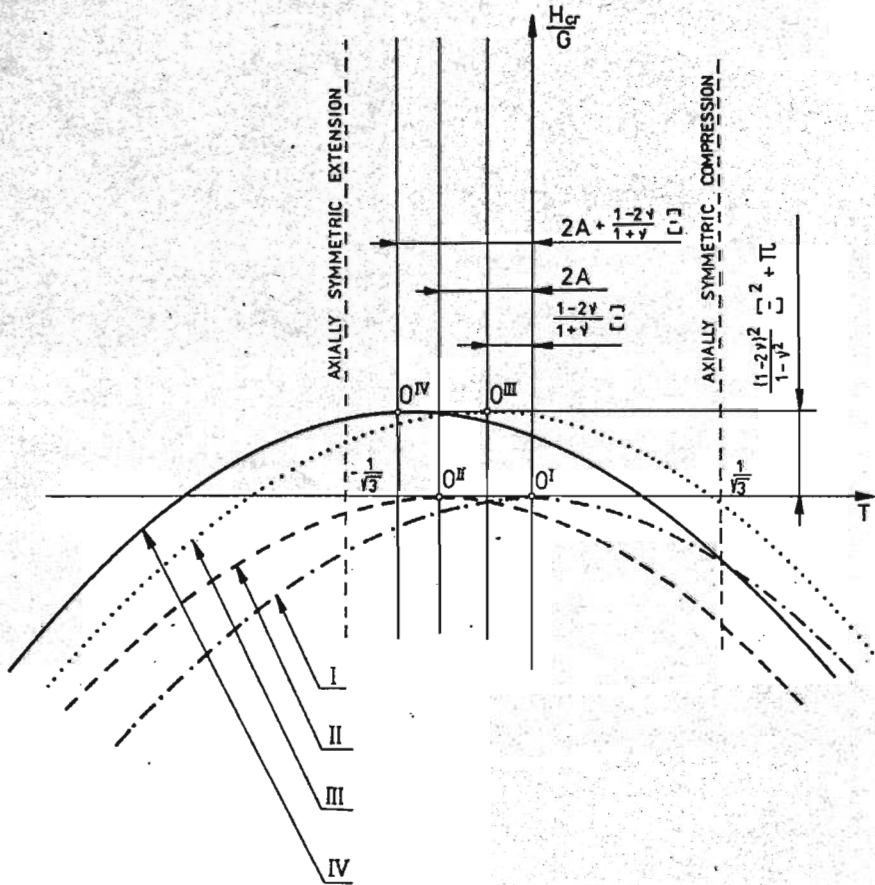
The results (4.31)<sub>1</sub> for the critical hardening modulus rate  $\frac{H_G}{G}$  as function of the state of stress  $T$  may be represented by the parabola IV (cf. Fig. 3). This parabola when compared with the parabola I (for  $A = 0, \Xi = 0$  and  $\Pi = 0$ ) is translated up by  $\frac{(1-2\nu)^2}{1-\nu^2}\Xi^2 + \Pi$  and is shifted left by  $2A + \frac{1-2\nu}{1+\nu}\Xi$ . The translation up is caused by both thermal effects, i.e. by thermal expansion (represented by  $\Xi$ ) and thermal plastic softening (represented by  $\Pi$ ), while the shifting left is implied by thermal expansion and the micro-damage process. The translation up means that the material is more inclined to instability by localization along the shear band and the shifting left shows that the inclination to instability for the axially symmetric compression is different from that for the axially symmetric tension. For tension material is more sensitive to localization than for compression.

The experimental results concerning the shear band localization phenomenon reported by ANAND and SPITZIG [1980] can be properly explained by considering the influence of thermo-mechanical couplings and the micro-damage effects.

## 5. Thermodynamic inelastic flow process

**5.1 Constitutive modelling for postcritical behaviour.** When the localization of plastic deformation along the shear band takes place the process considered for an entire body is no longer adiabatic.

Similarly as previously the isotropic hardening-softening and the strain induced anisotropy are incorporated in a model, the first by postulating the material function for  $\kappa$  and the second by introducing the back stress tensor  $\alpha$  as the internal state variable. The micro-damage process is described by using the internal state variable  $\xi$  interpreted as porosity or volume fraction parameter.



$$I \quad \frac{H_{cr}}{G} = -\frac{1+\nu}{2} T^2$$

$$II \quad \frac{H_{cr}}{G} = -\frac{1+\nu}{2} (T + 2A)^2$$

$$III \quad \frac{H_{cr}}{G} = -\frac{1+\nu}{2} \left( T + \frac{1-2\nu}{1+\nu} \Sigma \right)^2 + \frac{(1-2\nu)^2}{1-\nu^2} \Sigma^2 + \pi$$

$$IV \quad \frac{H_{cr}}{G} = -\frac{1+\nu}{2} \left( T + 2A + \frac{1-2\nu}{1+\nu} \Sigma \right)^2 + \frac{(1-2\nu)^2}{1-\nu^2} \Sigma^2 + \pi$$

Fig. 3



The intrinsic state is again defined by  $s$  (cf.(4.14)) and the internal state vector  $\mu$  by (4.6).

The viscoplastic flow rule for damaged solid is assumed in the form

$$d^P = \frac{\lambda}{\beta} \langle \Phi(f - \kappa) \rangle P, \quad P = \frac{1}{2\sqrt{J_2}} \frac{\partial f}{\partial \tau}. \quad (5.1)$$

The symbol  $\langle \Phi(f - \kappa) \rangle$  is defined as follows

$$\langle \Phi(f - \kappa) \rangle = \begin{cases} 0 & \text{if } f - \kappa \leq 0 \\ \Phi(f - \kappa) & \text{if } f - \kappa > 0, \end{cases}$$

and  $\lambda$  denotes the viscosity coefficient,  $\beta$  is the control function. The viscoplastic overstress function  $\Phi$  can be determined basing on available experimental results for dynamic loading processes.

It is noteworthy that the experimental form for  $\Phi$  is suggested by the physical consideration of the thermally - activated mechanism on crystalline slip systems.

The evolution equation for the internal state vector  $\mu$  has now the form

$$L_v \mu = m(s) \frac{\lambda}{\beta} \langle \Phi(f - \kappa) \rangle, \quad (5.3)$$

where the material function  $m(s)$  is determined by Eq.(4.13)<sub>6</sub>.

**5.2 Thermomechanical couplings.** Taking advantage of the results obtained in the previous papers of the author (cf.PERZYNA [1989]) and the evolution equation for the internal state vector assumed (5.3) we get the following set of two equations describing the thermo-mechanical properties during the thermodynamic process in the shear band region

$$\begin{aligned} L_v \tau &= \mathcal{L}^e \cdot d - \mathcal{L}^{th} \dot{\vartheta} - \frac{\lambda}{\beta} \langle \Phi(f - \kappa) \rangle \mathcal{L}^e \cdot P, \\ \rho c_p \dot{\vartheta} &= \text{div}(k \text{grad} \vartheta) + \rho \chi \frac{\lambda}{\beta} \langle \Phi(f - \kappa) \rangle, \end{aligned} \quad (5.4)$$

where  $\chi$  is given by Eq.(4.19).

**5.3 Formulation of the process.** For a thermodynamic viscoplastic flow process in the shear band region the mapping  $T_{(\cdot)}^{**}$  is defined by the initial - boundary - value problem as follows:

Find  $\varphi = (\phi, v, \vartheta, \mu)$  as function of  $x$  and  $t$  such that

(i) the field equations

$$\begin{aligned} \rho_{Ref} \dot{v} &= \operatorname{div} \tau, \\ L_v \tau &= \mathcal{L}^e \cdot d - \mathcal{L}^{th} \dot{\vartheta} - \frac{\lambda}{\beta} \langle \Phi(f - \kappa) \rangle \mathcal{L}^e \cdot P, \\ L_v \mu &= m(s) \frac{\lambda}{\beta} \langle \Phi(f - \kappa) \rangle, \\ \rho_{cp} \dot{\vartheta} &= \operatorname{div}(k \operatorname{grad} \vartheta) + \rho \chi \frac{\lambda}{\beta} \langle \Phi(f - \kappa) \rangle; \end{aligned} \quad (5.5)$$

(ii) the boundary conditions

tractions  $(\tau \cdot n)^a$  are prescribed on  $\partial B$ ,

temperature  $\vartheta$  is prescribed on  $\partial B$ ;

(iii) the initial conditions

$\phi, v, \vartheta$  and  $\mu$  are given at  $x \in B$  at  $t = \tau_c$ ; are satisfied.

## 6 Final failure along the shear band region

**6.1 Failure phenomenon along the shear band.** As it was observed experimentally (cf. GREBE, PAK and MAYERS [1985] and CHO, CHI and DUFFY [1988]) the onset of fracture along the shear band is directly related to the coalescence of ellipsoidal microcracks. From then on the microcrack coalescence and growth along the shear band result in the elongated macrocracks (cavities). The final failure occurs when one the most developed elongated macrocrack starts to propagate along the damaged shear band region.

**6.2 Criterion of fracture.** When the micro-damage process within the shear band region is sufficiently advanced the coalescence of microcracks begins.

During the dynamic process it is very difficult to control plastic deformation for different stages. Therefore it seems natural to base a criterion for coalescence and fracture on the control of porosity  $\xi$ .

Let denote by  $\xi^c$  a value of porosity at which the coalescence of microcracks begins and by  $\xi^F$  a value of porosity at fracture along the shear band region.

If porosity  $\xi$  is treated as a main parameter of the process (which can be controlled at every stage of the process), then the interval  $[\xi^c, \xi^F]$  represents the final mechanism of fracture. During this interval (i.e.  $\xi \in [\xi^c, \xi^F]$ ) the coalescence of microcracks plays a dominating role.

It is postulated that the fracture phenomenon occurs when

$$\xi = \xi^F \implies \epsilon^P = \epsilon_F^P(\dot{\epsilon}^P, \vartheta), \quad (6.1)$$

what leads to the condition

$$\kappa = \tilde{\kappa}(\epsilon^P, \xi, \vartheta) \left| \begin{array}{l} \xi = \xi^F \\ \epsilon^P = \epsilon_F^P \end{array} \right. = 0. \quad (6.2)$$

The condition (6.2) expresses the fact that fracture means a catastrophe or the intrinsic failure when the material along the shear band region loses its stress carrying capacity.

It is noteworthy that in the previous paper of the author (cf. PERZYNA [1987]) the directional character of the micro-damage process has been described by introducing an additional set of the internal state variables.

Taking advantage of this idea a simple micromechanical model of final failure has been proposed. The main conception of the model is based on the experimental observation that the coalescence of microcracks can be treated as nucleation and growth processes on a smaller scale. This gives very simple description of the propagation of a macrocrack in the damaged region along the shear band.

## 7 Final comments

The theory of shear band localization failure has been inspired by the important recent experimental investigations presented by GREBE, PAK and MEYERS [1985], HARTLEY, DUFFY and HAWLEY [1987], MARCHAND and DUFFY [1988], MARCHAND, CHO and DUFFY [1988] and CHO, CHI and DUFFY [1988].

All these experimental works have brought deep understanding of the shear band localization phenomenon and have given investigations of such cooperative phenomenon as the micro-damage process and the temperature dependent final mechanism of failure. They have emphasized the importance of the thermo-mechanical coupling effects and the strain rate sensitivity of a material. These works have also presented many important measurements and observations needed for the development of the theoretical descriptions.

It is hoped that the new theory of shear band localization failure is sufficiently simple in its nature that it can be applicable to the solution of technological, practical problems.

On the other hand this theory describes the most important cooperative phenomena such as the inelastic flow process, the instability of the flow process along localized shear band, the micro-damage process which consists of the nucleation, growth and coalescence of microcracks and the final mechanism of failure modelled by the propagation of an elongated macrocrack in the damaged shear band region.

The theory presented has some advantages. First, it includes in the consideration many important effects such as thermo-mechanical coupling, the strain rate sensitivity of a material and different kinds of the induced anisotropy. Second, it clearly distinguishes the response of the shear band region from the behaviour of a matrix global body. Third, it is consistent theory in a sense that each model developed describes different response of the same material according to different conditions superposed.

The theory proposed has been developed within the framework of the rate constitutive structure with internal state variables. The crucial idea is the efficient interpretation of the internal state variables introduced. This permits to base all considerations on good physical foundations and to utilize available experimental observations.



The application of the theory proposed may be expected in several technological processes such as dynamic fragmentation, high velocity machining, dynamic shaping and forming and low-temperature deformation processes.

#### REFERENCES

1. L.Anand and W.A.Spitzig, Initiation of localized shear band in plane strain, *J.Mech. Phys. Solids*, 28, 113-128 (1980).
2. K.Cho, Y.C.Chi, J.Duffy, Microscopic observations of adiabatic shear bands in three different steels, Brown University Report, September 1988.
3. M.K.Duszek, P.Perzyna, Plasticity of damaged solid and shear band localization, *Ing. Archiv* 58, 380-392 (1988).
4. M.K.Duszek, P.Perzyna, Influence of the kinematic hardening in the plastic flow localization in damaged solids, *Arch. Mechanics* 40, 595-609 (1988).
5. M.K.Duszek, P.Perzyna, On combined isotropic and kinematic hardening effects in plastic flow processes, *Int. J. Plasticity*, 1989 (in print).
6. M.K.Duszek, P.Perzyna, The localization of plastic deformation in thermo-plastic solids, *Int. J.Solids Structures*, 1989 (in print).
7. M.K.Duszek, P.Perzyna, E.Stein, Adiabatic shear band localization in elastic-plastic damaged solids, *The Second Int. Symp. Plasticity and its Current Applications*, July 31 - August 4, 1989, Mie University, Tsu, Japan.
8. H.A.Grebe, H.R.Pak, M.A.Meyer, Adiabatic shear localization in titanium and Ti-6 Pct Al-4 Pct V alloy, *Metall. Trans.* 16A, 761-775 (1985).
9. A.L.Gurson, Continuum theory of ductile rupture by void nucleation and growth, Part I. Yield criteria and flow rules for porous ductile media, *J.Eng.Mater. Technol.* 99, 2-15 (1977).
10. K.A.Hartley, J.Duffy, R.H.Hawley, Measurement of the temperature profile during shear band formation in steels deforming at high strain rates, *J.Mech. Phys. Solids* 35, 283-301 (1987).



11. K.Ikegami, Experimental plasticity on the anisotropy of metals, Proc. Euro-mech Colloquium 115, Mechanical Behaviour of Anisotropic Solids, Ed. J.P. Boehler, pp.201-242 (1982).
12. J.N. Johnson, Dynamic fracture and spallation in ductile solids, J. Appl. Phys. 52, 2812-2825 (1981).
13. A.Marchand, J.Duffy, An experimental study of the formation process of adiabatic shear bands in a structural steel, J.Mech.Phys. Solids 36, 251-283 (1988).
14. A.Marchand, K.Cho, J.Duffy, The formation of adiabatic shear bands in an AISI 1018 cold-rolled steel, Brown University Report, September 1988.
15. M.A.Meyer, C.T. Aimone, Dynamic fracture (spalling) of metals, Prog. Mater. Sci 28, 1-96 (1983).
16. Y.Nakayama and K.Mori, Microstructure and shear band formation in rolled single crystals of Al - Mg alloy, Acta Metall., 35, 1747-1755 (1987).
17. J.A. Nemes, J. Eftis, P.W. Randles, Viscoplastic constitutive modeling of high strain-rate deformation, material damage and spall fracture, Manuscript 1988, in print.
18. A.Neddleman, J.R. Rice, Limits to ductility set by plastic flow localization, in Mechanics of Sheet Metal Forming (ed. D.P. Koistinen and N.-M. Wang), Plenum, New York 1978, 237-267.
19. J. Pan, J.R. Rice, Rate sensitivity of plastic flow and implications for yield surface vertices, Int. J. Solids Structures 19, 973-987 (1983).
20. P. Perzyna, The constitutive equations for rate sensitive plastic materials, Quart. Appl. Math. 20, 321-332 (1963).
21. P. Perzyna, Fundamental problems in viscoplasticity, Advances in Applied Mechanics 9, 243-377 (1966).
22. P. Perzyna, Thermodynamic theory of viscoplasticity, Advances in Applied Mechanics 11, 313-354 (1971).

23. P. Perzyna, Coupling of dissipative mechanisms of viscoplastic flow, *Arch. Mechanics* 29, 607-624 (1977).
24. P. Perzyna, Thermodynamics of dissipative materials, in *Recent Developments in Thermomechanics of Solids*, Eds. G. Lebon and P. Perzyna, Springer, Wien, 95-220 (1980).
25. P. Perzyna, Modified theory of viscoplasticity, Application to advanced flow and instability phenomena, *Arch. Mechanics* 32, 403-420 (1980).
26. P. Perzyna, Stability of flow processes for dissipative solids with internal imperfections, *ZAMP* 35, 848-867 (1984).
27. P. Perzyna, Constitutive modelling of dissipative solids for postcritical behaviour and fracture, *ASME J. Engng. Mater. Technol* 106, 410-419 (1984).
28. P. Perzyna, Dependence of fracture phenomena upon the evolution of constitutive structure of solids, *Arch. Mechanics* 37, 485-501 (1985).
29. P. Perzyna, Constitutive modelling for brittle dynamic fracture in dissipative solids, *Arch. Mechanics* 38, 725-738 (1986).
30. P. Perzyna, Internal state variable description of dynamic fracture of ductile solids, *Int. J. Solids Structure* 22, 797-818 (1986).
31. P. Perzyna, Temperature and rate dependent theory of plasticity of crystalline solids, *Revue de Physique Appliquee* 23, 445-459 (1988).
32. P. Perzyna, Influence of anisotropic effects on micro-damage processes in dissipative solids, *IUTAM/ICM Symposium on Yielding, Damage and Failure of Anisotropic Solids*, Villard-de-Lans, August 1987, Proc. (in print).
33. P. Perzyna, Temperature and rate dependent theory of plasticity of polycrystalline solids, *The second Int. Symp. Plasticity and its current Applications*, July 31 - August 4, 1989, Mie University, Tsu, Japan.
34. P. Perzyna, Constitutive equations of dynamic plasticity, *Engineering Application of Modern Plasticity*, Post Symposium Short Course, August 4-5, 1989, Nagoya, Japan.

35. A. Phillips, W.-Y. Lu, An experimental investigation of yield surfaces and loading surfaces of pure aluminium with stress-controlled and strain-controlled paths of loading, *ASME J. Eng. Mater. Technol.* 106, 349-354 (1984).
36. W. Prager, The theory of plasticity: a survey of recent achievements, (J. Clayton Lecture), *Proc. Inst. Mech. Eng.* 169, 41 (1955).
37. J.R. Rice, The localization of plastic deformation, *Theoretical and Applied Mechanics*, ed. W.T. Koiter, North-Holland, 207-220 (1976).
38. J.R. Rice, Continuum mechanics and thermodynamics of plasticity in relation to microscale deformation mechanisms, in *Constitutive Equations in Plasticity*, (ed. A.S. Argon), The MIT Press, Cambridge, 23-75 (1975).
39. J.R. Rice, J.W. Rudnicki, A note on some features of the theory of localization of deformation, *Int. J. Solids Structures* 16, 597-605 (1980).
40. H.C. Rogers, C.V. Shastri, Material factors in adiabatic shearing in steels, in *Shock Waves and High-Strain-Rate Phenomena in Metals*, (eds. M.A. Meyers and L.E. Murr), Plenum, 285-298 (1981).
41. J.W. Rudnicki, J.R. Rice, Conditions for the localization of deformation in pressure - sensitive dilatant materials, *J. Mech. Phys. Solids* 23, 371-394 (1975).
42. M. Saje, J. Pan, A. Needleman, Void nucleation effects on shear localization in porous plastic solids, *Int. J. Fracture* 19, 163-182 (1982).
43. D.A. Shockey, L. Seaman, D.R. Curran, The micro-statistical fracture mechanics approach to dynamic fracture problems, *Int. J. Fracture* 27, 145-157 (1985).
44. V. Tvergaard, Effects of yield surface curvature and void nucleation on plastic flow localization, *J. Mech. Phys. Solids* 35, 43-60 (1987).
45. V. Tvergaard, A. Needleman, Effect of material rate sensitivity on failure modes in the Charpy V-notch test, *J. Mech. Phys. Solids* 34, 213-241 (1986).

46. A.T. Yokobori Jr., T. Yokobori, K. Sato, K. Syoji, Fatigue crack growth under mixed modes I and II, *Fatigue Fract. Mater. Struct.* 8, 315-325 (1985).
47. H. Ziegler, A modification of Prager's hardening rule, *Quart. Appl. Math.* 17, 55-65 (1959).

### EFEKTY TERMICZNE W ZNISZCZENIU POPRZEDZONYM LOKALIZACJĄ WZDŁUŻ ADIABATYCZNYCH PASM ŚCINANIA

Celem pracy jest opis wpływu efektów termicznych na zniszczenie poprzedzone lokalizacją wzdłuż pasm ścinania. Ten rodzaj zniszczenia jest ogólnie wiązany z plastyczną niestabilnością spowodowaną termicznym osłabieniem podczas dynamicznej deformacji. Wykorzystując analizę rezultatów doświadczalnych dla dynamicznych obciążeń pierwsza część procesu płynięcia jest traktowana jako adiabatyczna.

Wykorzystano model materiału termo-sprężysto-plastycznego z efektami wewnętrznych mikrouszkodzeń. Wzięto pod uwagę termo-mechaniczne sprzężenie. Zbadano kryterium lokalizacji plastycznych deformacji wzdłuż pasma poślizgu. Pokrytyczne zachowanie się materiału wzdłuż pasm ścinania modelowane jest termo-sprężysto-lepkoplastyczną reakcją z zaawansowanym procesem mikro-uszkodzenia. Obydwa modele są rozwinięte w ramach konstytutywnej struktury typu prędkościowego z parametrami wewnętrznymi. Zaproponowano dynamiczne kryterium zniszczenia wzdłuż pasm ścinania. Przedstawiono prosty mikromechaniczny model końcowego zniszczenia z uwzględnieniem efektów termicznych i anizotropowych.